Journal of Computer-Aided Molecular Design, 11 (1997) 278–292.

J-CAMD 393

Structure–activity relationships of cannabinoids: A joint CoMFA and pseudoreceptor modelling study

Silke Schmetzer[a], Paulette Greenidge[b], Karl-Artur Kovar[a,*], Meike Schulze-Alexandru[a] and Gerd Folkers[b]

[a]*Institute of Pharmacy, University of Tübingen, Auf der Morgenstelle 8, D-72076 Tübingen, Germany*
[b]*Department of Pharmacy, ETH Zürich, CH-8057 Zürich, Switzerland*

Received 6 May 1996
Accepted 23 December 1996

Keywords: Δ^9-Tetrahydrocannabinol; Pharmacophore; Molecular modelling; CADD; YAK

Summary

A cannabinoid pseudoreceptor model for the CB1-receptor has been constructed for 31 cannabinoids using the molecular modelling software YAK. Additionally, two CoMFA studies were performed on these ligands, the first of which was conducted prior to the building of the pseudoreceptor. Its pharmacophore is identical with the initial superposition of ligands used for pseudoreceptor construction. In contrast, the ligand alignment for the second CoMFA study was taken directly from the final cannabinoid pseudoreceptor model. This altered alignment gives markedly improved cross-validated r^2 values as compared to those obtained from the original alignment with r^2_{cross} values of 0.79 and 0.63, respectively, for five components. However, the pharmacophore alignment has the better predictive ability. Both the CoMFA and pseudoreceptor methods predict the free energy of binding of test ligands well.

Introduction

Cannabis preparations, such as marihuana and hashish, have been used for centuries on account of both their psychotropic and pharmacological effects. (6a*R*,10a*R*)-Δ^9-Tetrahydrocannabinol (**1**, Δ^9-THC, Fig. 1), the psychotropic component of cannabis preparations [1], also exhibits anti-emetic, analgesic, muscle-relaxing, blood-pressure-reducing, bronchodilating effects and reduces pathologically elevated intraocular pressure (glaucoma) [2–6]. In all probability, the analgesic and the psychotropic effects are mediated through the central cannabinoid receptor (CB1); however, almost nothing is known, as yet, concerning signal transduction pathways of the other pharmacological effects [2,7,8]. The pharmacological effects have led to the synthesis of other cannabinoids. The synthetic analogues are referred to as non-classical cannabinoids and differ from the classical cannabinoids in the absence of the tetrahydropyran ring [9,10]. The essential structural prerequisites for ligand–receptor interaction of the cannabinoids are the free phenolic hydroxyl group [11] and the alkyl side chain at ring A [2]. Extension and branching of the pentyl side chain of Δ^9-THC yields the dimethylheptyl (DMH) derivative with a greatly increased affinity for the cannabinoid receptors [2,12]. Within the non-classical cannabinoids, increasing the length of the DMH side chain to 9–11 C atoms and shortening it to ≤6 C atoms leads to a reduction of the affinity [13]. While an alcoholic hydroxyl group at C-9 or C-11 is not essential, although it increases the activity in the case of classical cannabinoids, structure–activity relationship studies reveal that the hydroxyl group at ring C is essential for the analgesic activity in the case of non-classical cannabinoids [14]. Furthermore, Reggio et al. [15] have reported a receptor essential volume near the top of the C ring in the bottom face of the molecule. Although the pharmacological activity and the structure–effect relationships are well documented [14,16], almost nothing is known about the ligand–receptor interaction at the molecular level. The identification [17] and cloning [18] of the cannabinoid receptor in the brain (CB1) and the characterization of the peripheral cannabinoid receptor (CB2) [19] have provided a new impulse for the investigation of the molecular basis of the ligand–receptor interac-

*To whom correspondence should be addressed.

tion. It has, as yet, not proved possible to isolate the pure membrane-bound, G-protein-coupled cannabinoid receptor in crystalline form. This is a prerequisite for structural elucidation using X-ray structural analysis and nuclear magnetic resonance methods; thus, the three-dimensional structure of this receptor is still unknown. In spite of the lack of knowledge of the three-dimensional structure of the receptor, it ought to be possible to use a computer-aided drug design (CADD) model to make predictions concerning the quantitative structure–effect relationships on the basis of the known properties of an ensemble of ligands of the unknown receptor.

Materials and Methods

Selection of the cannabinoids

The training set consisted of 29 cannabinoids (Fig. 1) for which binding data were available from one study [7]. The radioligand binding study by Compton et al. [7], used as a basis, involved determination of the binding affinities of 59 cannabinoids with the radioligand (^{3}H)-CP-55,940 (Table 1) at the central receptor (CB1) of the rat (K_i values). On the basis of a good correlation between K_i values <800 nM and in vivo activity, 31 cannabinoids with K_i values <800 nM were chosen as the training set for compilation of the pharmacophore, the pseudoreceptor model and the CoMFA model. The only compounds excluded from the training set were 1',2'-dimethylheptylpyran($\Delta^{6a,10a}$), on account of the lack of information concerning its stereochemistry, and **7** which was used as a test ligand. Additionally, **31**, with a $K_i > 800$ nM, was also used as a test ligand. (The designation of the non-classical bicyclic cannabinoids with Roman numerals has been adopted from earlier studies [7,20].)

Molecular modelling

Calculations were carried out on an SGI Indigo XS24 workstation. The structures of the cannabinoids were constructed using the molecular modelling program SYBYL 6.0 and 6.03 (Tripos Associates Inc., St. Louis, MO, U.S.A.) and further refined. The crystal structures were loaded into SYBYL from the Cambridge Crystallographic Database [21] with the aid of the Crysin option. Geometrical optimization of all structures was carried out with MAXIMIN2. MOPAC charges were calculated with the aid of the semiempirical, quantum-chemical procedure AM1 (MOPAC 5.0 [22]). Systematic conformation analyses were carried out using the Search Routine within the SYBYL program package. During the conformational analysis, those bonds capable of rotation were rotated through 360° in steps of 1° or 5°. Conformations whose energies were not more than 15 kcal/mol above that of the lowest energy conformation were accepted as energetically permitted. The evaluation of the energetically permitted conformations of the systematic conformation analysis was carried out using the programs Starmaker and Starcompare [23]. During the conformational analysis, the side chain was fixed in the all anti conformation regarded as being of minimum energy (see the section 'Pharmacophore'). It is known from X-ray diffraction analysis and the data of NMR spectroscopy that rings B and C of Δ^9-THC and Δ^8-THC derivates take up a half-chair conformation [24,25] and ring C of $\Delta^{9,11}$-THC derivates takes up a chair conformation (ring B also a half-chair conformation) [26]. These ring conformations were constructed and used in further calculations. No X-ray structure analysis data are available concerning compounds **4**, **5**, **17** and **18**. The semirigid cyclohexane ring (ring C) of these compounds was constructed in boat and chair conformation; both of the two possible conformations were then used in further calculations (see the section 'Pharmacophore').

Pharmacophore

The free phenolic hydroxyl group and the alkyl side chains on ring A were defined as pharmacophoric groups on the basis of structure–effect relationships. Systematic conformation analysis was used to seek a common spatial orientation of these pharmacophoric groups amongst the energetically permitted conformations. The side chain essential for the activity was set in the all anti conformation regarded as being of minimum energy. This orientation of the side chain was chosen arbitrarily since no information is available from X-ray data concerning its actual conformation at the binding site. Hence, the results concerning the side chains in this study must not be regarded as being absolute with respect to the activity-relevant orientation, but rather as being relatively dependent in activity on the length and/or branching of the side chain. The rigid and simultaneously most active compound **15** was chosen as template for limitation of the conformation volume of flexible molecules. The SYBYL-implemented multifit routine was used to fit the flexible molecules, with simultaneous optimization of the geometry, to the rigid template **15**, that was defined as an aggregate, with the intention of reaching a spatial correspondence between the pharmacophoric structural elements of the template and the flexible molecule. For this purpose, a spring constant of 20 kcal/mol was applied between atoms whose positions were to correspond. In order to fulfil the steric requirements at position C-9 of the classical cannabinoids and at C-1 of the non-classical cannabinoids, the energetically permitted conformation, whose C-9 (classical cannabinoids) or C-1 substituent (non-classical cannabinoids) corresponded spatially with that of the very active classical cannabinoid **15**, was chosen as the effective conformation. In the case of the non-classical cannabinoids that bore an essential hydroxyl group at C-1, the spatial correspondence of this hydroxyl group with the non-essential but effect-amplifying hydroxyl group at C-

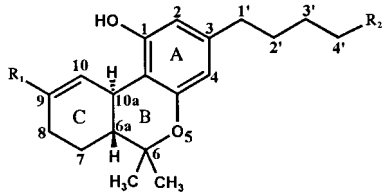

Structure		Abbreviation	R_1	R_2
1	(6a*R*,10a*R*)-Δ^9-Tetrahydrocannabinol	Δ^9-THC	CH_3	CH_3
2	(6a*R*,10a*R*)-5'-Hydroxy-Δ^9-tetrahydrocannabinol	5'-OH-Δ^9-THC	CH_3	CH_2OH
3	(6a*R*,10a*R*)-11-Hydroxy-Δ^9-tetrahydrocannabinol	11-OH-Δ^9-THC	CH_2OH	CH_3

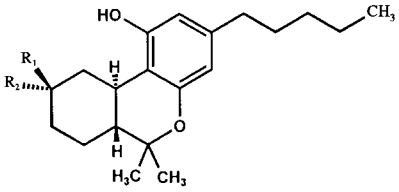

Structure		Abbreviation	R_1	R_2
4	(6a*R*,9*R*,10a*R*)-9β-Hydroxy-hexahydrocannabinol	9β-OH-HHC	CH_3	OH
5	(6a*R*,9*S*,10a*R*)-9α-Hydroxy-hexahydrocannabinol	9α-OH-HHC	OH	CH_3
16	(6a*R*,10a*R*)-$\Delta^{9,11}$-Tetrahydrocannabinol	$\Delta^{9,11}$-THC	$=CH_2$	$=CH_2$

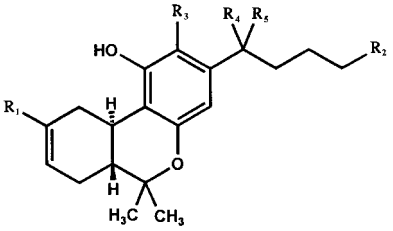

Structure		Abbreviation	R_1	R_2	R_3	R_4	R_5
6	(6a*R*,10a*R*)-Δ^8-Tetrahydrocannabinol	Δ^8-THC	CH_3	CH_3	H	H	H
7	(6a*R*,10a*R*)-5'-Brom-Δ^8-tetrahydrocannabinol	5'-Br-Δ^8-THC	CH_3	CH_2Br	H	H	H
8	(6a*R*,10a*R*)-5'-Iod-Δ^8-tetrahydrocannabinol	5'-I-Δ^8-THC	CH_3	CH_2I	H	H	H
9	(6a*R*,10a*R*)-5',5',5'-Trifluor-Δ^8-tetrahydrocannabinol	5'-F_3-Δ^8-THC	CH_3	CF_3	H	H	H
10	(6a*R*,10a*R*)-5'-Fluor-Δ^8-tetrahydrocannabinol	5'-F-Δ^8-THC	CH_3	CH_2F	H	H	H
11	(6a*R*,10a*R*)-2-Iod-Δ^8-tetrahydrocannabinol	2-I-Δ^8-THC	CH_3	CH_3	I	H	H
12	(6a*R*,10a*R*)-11-Fluor-Δ^8-tetrahydrocannabinol	11-F-Δ^8-THC	CH_2F	CH_3	H	H	H
13	(6a*R*,10a*R*)-11-Hydroxy-Δ^8-tetrahydrocannabinol	11-OH-Δ^8-THC	CH_2OH	CH_3	H	H	H
14	(6a*R*,10a*R*)-3-(1,1-Dimethylheptyl)-Δ^8-tetrahydrocannabinol	Δ^8-THC-DMH	CH_3	CH_3	H	CH_3	CH_3
15	(6a*R*,10a*R*)-11-Hydroxy-3-(1,1-dimethylheptyl)-Δ^8-tetrahydrocannabinol	11-OH-Δ^8-THC-DMH	CH_2OH	CH_3	H	CH_3	CH_3

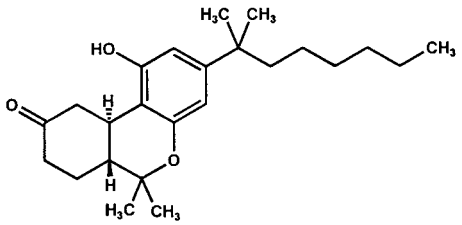

Structure
17 Nabilone

Fig. 1. Structural formula of the cannabinoids: **1**–**18**, classical cannabinoids; **19**–**31**, non-classical cannabinoids.

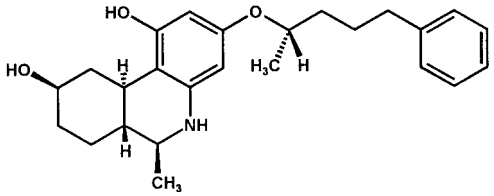

Structure	Abbreviation
18 Desacetyllevonantradol	DALN

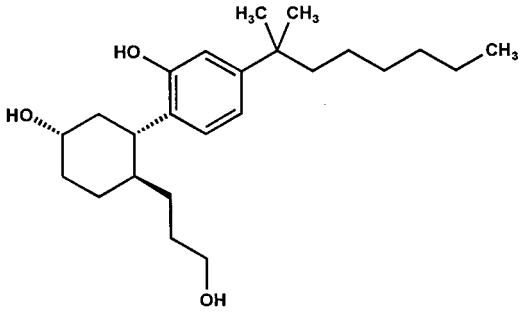

Structure	Abbreviation
29 1*S*,3*S*,4*S*)-3-[2-Hydroxy-4-(1,1-dimethylheptyl)-phenyl]-4-(3-hydroxypropyl)-cyclohexan-1-ol	CP-56,667; XV

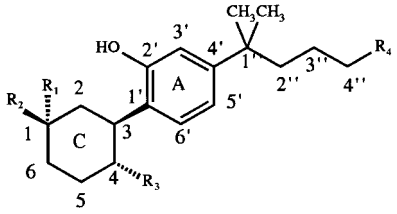

Structure	Abbreviation	R_1	R_2	R_3	R_4
19 (1*R*,3*S*)-3-[2-Hydroxy-4-(1,1-dimethylpentyl)-phenyl]-cyclohexan-1-ol	IV	H	OH	H	CH_3
20 (1*R*,3*S*)-3-[2-Hydroxy-4-(1,1-dimethylhexyl)-phenyl]-cyclohexan-1-ol	V	H	OH	H	C_2H_5
21 (1*R*,3*S*)-3-[2-Hydroxy-4-(1,1-dimethylheptyl)-phenyl]-cyclohexan-1-ol	CP-47,497; VI	H	OH	H	C_3H_7
22 (1*R*,3*S*)-3-[2-Hydroxy-4-(1,1-dimethyloctyl)-phenyl]-cyclohexan-1-ol	VII	H	OH	H	C_4H_9
23 (1*R*,3*S*)-3-[2-Hydroxy-4-(1,1-dimethylnonyl)-phenyl]-cyclohexan-1-ol	VIII	H	OH	H	C_5H_{11}
24 (1*R*,3*S*)-3-[2-Hydroxy-4-(1,1-dimethyldexyl)-phenyl]-cyclohexan-1-ol	IX	H	OH	H	C_6H_{13}
25 (1*R*,3*S*)-3-[2-Hydroxy-4-(1,1-dimethyldodexyl)-phenyl]-cyclohexan-1-ol	X	H	OH	H	C_7H_{15}
26 (1*S*,3*R*,4*R*)-3-[2-Hydroxy-4-(1,1-dimethylheptyl)-phenyl]-4-methyl-cyclohexan-1-ol	XI	OH	H	CH_3	C_3H_7
27 (1*R*,3*R*,4*R*)-3-[2-Hydroxy-4-(1,1-dimethylheptyl)-phenyl]-4-methyl-cyclohexan-1-ol	XII	H	OH	CH_3	C_3H_7
28 (1*R*,3*R*,4*R*)-3-[2-Hydroxy-4-(1,1-dimethylheptyl)-phenyl]-4-(3-hydroxypropyl)-cyclohexan-1-ol	CP-55,940	H	OH	C_3H_6OH	C_3H_7
30 (1*R*,3*R*,4*R*)-3-[2-Hydroxy-4-(1,1-dimethylheptyl)-phenyl]-4-(4-hydroxybutyl)-cyclohexan-1-ol	XVI	H	OH	C_4H_8OH	C_3H_7

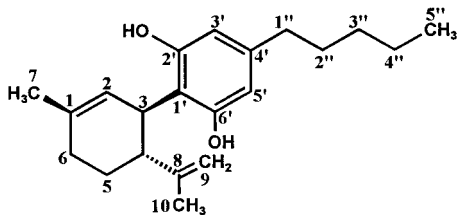

Structure	Abbreviation
31 Cannabidiol	CBD

Fig. 1. (continued).

TABLE 1
K_i VALUES

Ligand	K_i (nM)	±SE	$\Delta G_{exp.}$ (kcal/mol)	Deviation from $\Delta G_{exp.}$ (kcal/mol)
15	0.728	0.113	−12.962	−13.065 ≥ −12.962 ≥ −12.873
28	0.924	0.140	−12.815	−12.916 ≥ −12.815 ≥ −12.728
18	1.06	0.24	−12.730	−12.888 ≥ −12.730 ≥ −12.604
30	1.55	0.85	−12.496	−12.986 ≥ −12.496 ≥ −12.227
14	1.59	0.24	−12.480	−12.581 ≥ −12.480 ≥ −12.394
22	4.73	1.34	−11.809	−12.014 ≥ −11.809 ≥ −11.655
26	6.15	1.99	−11.647	−11.888 ≥ −11.647 ≥ −11.474
7	7.63	1.41	−11.514	−11.640 ≥ −11.514 ≥ −11.410
27	7.70	2.05	−11.509	−11.699 ≥ −11.509 ≥ −11.363
8	7.77	2.40	−11.503	−11.731 ≥ −11.503 ≥ −11.337
21	9.54	0.35	−11.377	−11.400 ≥ −11.377 ≥ −11.354
9	19.9	0.9	−10.924	−10.952 ≥ −10.924 ≥ −10.896
17	22.3	6.6	−10.854	−11.070 ≥ −10.854 ≥ −10.694
23	28.5	3.3	−10.702	−10.778 ≥ −10.702 ≥ −10.635
3	38.4	0.8	−10.519	−10.532 ≥ −10.519 ≥ −10.506
1	40.7	1.7	−10.483	−10.509 ≥ −10.483 ≥ −10.458
13	54.9	10.2	−10.299	−10.425 ≥ −10.299 ≥ −10.194
10	57.0	2.3	−10.275	−10.301 ≥ −10.275 ≥ −10.251
29	61.7	5.0	−10.227	−10.279 ≥ −10.227 ≥ −10.179
2	87.6	6.4	−10.011	−10.057 ≥ −10.011 ≥ −9.967
11	89.0	15.5	−10.001	−10.119 ≥ −10.001 ≥ −9.902
12	107	28	−9.887	−10.074 ≥ −9.887 ≥ −9.744
4	124	11	−9.797	−9.854 ≥ −9.797 ≥ −9.744
20	126	9	−9.787	−9.832 ≥ −9.787 ≥ −9.744
6	126	16	−9.787	−9.870 ≥ −9.787 ≥ −9.713
24	163	35	−9.628	−9.777 ≥ −9.628 ≥ −9.508
5	171	8	−9.599	−9.628 ≥ −9.599 ≥ −9.570
16	236	55	−9.400	−9.564 ≥ −9.400 ≥ −9.271
25	381	28	−9.105	−9.152 ≥ −9.105 ≥ −9.061
19	735	14	−8.700	−8.712 ≥ −8.700 ≥ −8.689
31	4350	390	−7.605	−7.663 ≥ −7.605 ≥ −7.552

11 of the most active compound **15** is a necessary condition for activity. This condition does not have to be fulfilled in the case of the classical cannabinoids whose C-9 substituent is not essential for activity; rather the C-9 substituent of the rigid and at the same time most active template **15** points to a permitted area for the C-9 substituent. Since this area is not necessarily the sole permitted area for the C-9 substituent of the classical cannabinoids, compounds that do not fulfil this spatial correspondence at C-9 or C-1 cannot yet provide any evidence concerning the conformation at the receptor. In such cases, the receptor essential volume according to Marshall was also included in order to make a decision [27–31]. Those conformations, that penetrate the receptor essential volume with a portion of their own volume, are inactive. For this purpose, the volume made available by the receptor (excluded volume) was first calculated as the common volume of active molecules in their active conformations. Then the additional volume (unique volume), that is not part of the common volume of all active molecules, was calculated for the inactive cannabinoids dextronantradol, (6a*S*,10a*S*)-11-OH-Δ^8-THC-DMH and (9*S*,6a*R*)-*trans*-$\Delta^{10,10a}$-THC. The intersection of the unique volumes of these inactive cannabinoids is designated as the receptor essential volume (REV). This region is in agreement with the REV determined by Reggio et al. [15]. If it was not possible to reach a decision by consideration of the pharmacophore or of the REV, then the CoMFA model was used to check the energetically possible conformations and the 'best' conformation was chosen (see the section 'CoMFA').

YAK

Based solely on the structures of known ligand molecules, the pseudoreceptor modelling method YAK (see Ref. 32 for a detailed description) aims to predict the relative free energies of binding for novel congeneric ligands. A pseudoreceptor model is one that mimics the essential ligand–macromolecule interactions of the biological receptor, the superimposed ligands serving as the receptor mapping template. The models are validated by their ability to reproduce the experimental data of the training set. The pharmacophoric alignment of the ligands as described above was used to generate the pseudorecep-

tor model. All calculations and visualizations were performed on an SGI Indigo XS24 or an SGI Indigo Extreme. Solvation energies (see below) were calculated semianalytically [33] with AM1 charges. Relative free energies of binding were calculated according to Eq. 1 [32],

$$\Delta(\Delta G^{\circ}_{calc.}) \cong \Delta(\Delta E_{calc.}) - \Delta(\Delta G_{solvation,ligand}) \quad (1)$$

where $\Delta E_{calc.}$ is the interaction energy between an individual ligand and the pseudoreceptor as calculated by YAK, and $\Delta G_{solvation,ligand}$ is the free energy of ligand solvation, and corrected by means of a linear regression (LR) between $\Delta(\Delta G^{\circ}_{calc.})$ and $\Delta(\Delta G^{\circ}_{exp.})$ according to Eq. 2,

$$\Delta(\Delta G^{\circ}_{corr.}) = slope^{LR}\, \Delta(\Delta G^{\circ}_{calc.}) \quad (2)$$

CoMFA

The CoMFA studies were carried out using the QSAR module integrated in the molecular modelling program SYBYL. The biological data were the free energies of binding ($\Delta G_{exp.}$), which can be derived from the K_i values [7] (Table 1) using the following equation: $\Delta G_{exp.} = -RT \ln K_i$ with T = 310 K. The lattice was so chosen that all three dimensions (x,y,z) each extended 5 Å beyond the largest molecules. The distance between lattice points was 2 Å. The probe atom was chosen to be an sp^3-hybridized carbon atom with a charge of +1. Atomic charges were calculated with AM1. The steric and electrostatic interactions between the probe atom and the cannabinoids were calculated. If probe atoms lying within or in the neighbourhood of a compound have interaction energies exceeding the cutoff value of 30 kcal/mol, then the interaction energy is replaced by this cutoff value. The statistical analysis of this complex data matrix was carried out by means of the partial least-squares (PLS) technique (scaling method: CoMFA standard; same weights for all; minimum sigma: 2.0 {cross-validation}, 0.0 {non-cross-validation}). The technique of leave-one-out cross-validation was used to check the results of this complex analysis. The final PLS analysis of the complete data set serves for the prediction of new compounds and for comparison with the pseudoreceptor model. The alignment of the first CoMFA analysis is based on the pharmacophore model and will be addressed below as 'pharmacophore alignment'; this CoMFA analysis served initially for the selection of effective conformations. The second CoMFA analysis was carried out with the new alignment resulting from the pseudoreceptor model. All evaluations were performed according to 'Recommendations for CoMFA Studies and 3D QSAR Publications' [34].

Results

Pharmacophore model, classical cannabinoids

The Δ^9-THC and Δ^8-THC derivatives of the classical cannabinoids were inferred from the crystal structure of Δ^9-THC acid [35,36]. The geometrically optimized structures are in close agreement with the structures obtained by NMR spectroscopy [24,37] and high-resolution NMR spectroscopy [26], with rings C and B in a half-chair conformation. The hexahydrocannabinol (HHC) derivatives **4** and **5** were inferred from the geometry-optimized crystal structure of the 3-methyl-HHC [21]. After calculation of all energetically permitted ring conformations, the energetically most probable conformation was found, in agreement with data from NMR spectroscopy [37] of the HHC tricycle, to involve ring B in the half-chair conformation and ring C in the chair conformation. In the case of **4**, this lowest energy conformation fulfils the structural requirements of the pharmacophore. In contrast, no match was obtained between the lowest energy conformation of **5** and the reference molecule; it was not possible to bring the OH group in position 9 into a spatial fit. A spatial fit of all three structural elements was obtained in the energetically less favourable conformation of **5** with ring C in a twist conformation. The application of receptor site mapping made it possible to exclude as an effective conformation the chair conformation of **5**, since part of the molecule projected into the REV. The lowest energy conformation of **16** with ring B in the half-chair conformation and ring C in the chair conformation is in agreement with data from high-resolution NMR spectroscopy [36]. A further energetically possible conformation with ring C in the twist conformation also fulfils the requirements for the pharmacophore. Both energetically possible conformations have no portion of the molecule projecting into the REV. Since it also proved impossible to decide between the two conformations of **16** on the basis of the CoMFA analysis, where both gave favourable predictions, the energetically most favourable conformation with ring C in the chair conformation was taken as the most probable conformation at the receptor. In the case of **17**, ring C can take the chair or twist conformation. Neither conformation penetrates the REV. On the basis of CoMFA analysis, the twist conformation was selected as the effective conformation since the deviation from the experimental value was least. Levonantradol, a prodrug, was modelled as active metabolite **18**. The cyclohexane ring of **18** lies in a chair conformation with the OH group at C-1 in an equatorial position.

Pharmacophore model, non-classical cannabinoids

The AC derivative **21** is a prototype for the class of non-classical cannabinoids. It is the simplest non-classical cannabinoid with all the structural elements necessary for the effect, namely the phenolic OH group at C-2', the side chain at C-4' and the OH group at C-1 [14]. According to 2D NMR data [38], the cyclohexane ring is present in the chair conformation with the OH group and the aromatic ring in the equatorial position. There are two conforma-

TABLE 2
COMPARISON OF YAK CALCULATED AND EXPERIMENTAL FREE BINDING ENERGIES OF CANNABINOIDS

Ligand	$\Delta G_{exp.}$ (kcal/mol)	$\Delta G_{corr.}$ (kcal/mol)	$\Delta G_{corr.} - \Delta G_{exp.}$ (kcal/mol)
Training set[a]			
15	*–12.962*	*–12.962*	*0.000*
28	–12.815	–13.010	–0.195
18	–12.730	–12.998	–0.268
30	–12.496	–12.825	–0.329
14	–12.480	–12.394	0.086
22	–11.809	–12.164	–0.355
26	–11.647	–11.319	0.328
27	–11.509	–11.056	0.453
8	–11.503	–11.509	–0.006
21	–11.377	–11.074	0.303
9	–10.924	–10.574	0.350
17	–10.854	–11.038	–0.184
23	–10.702	–11.429	–0.727
3	–10.519	–11.104	–0.585
1	–10.483	–10.041	0.442
13	–10.299	–10.696	–0.397
10	–10.275	–10.397	–0.122
29	–10.227	–10.876	–0.649
2	–10.011	–9.551	0.460
11	–10.001	–10.025	–0.024
12	–9.887	–9.988	–0.101
4	–9.797	–10.109	–0.312
20	–9.787	–10.258	–0.471
6	–9.787	–10.482	–0.695
24	–9.628	–9.756	–0.128
5	–9.599	–9.694	–0.095
16	–9.400	–9.818	–0.418
25	–9.105	–9.350	–0.245
19	–8.700	–9.511	–0.811
Test set			
7	–11.514	–11.028	0.486
31	–7.605	–4.022[b]	–3.583[b]
		–7.873[c]	–0.268[c]

The reference compound is designated by italics.
[a] The training set contains 29 ligands; r = 0.951.
[b] Superposition 1.
[c] Superposition 2.

tion minima with a torsional angle of ~60° or ~120° between the cyclohexane ring and the aromatic ring. These two lowest energy conformations could be confirmed with the computer by means of systematic conformation analysis and geometrical optimization; however, they do not fulfil the requirements for the pharmacophore. Rotation about the bond between the aromatic ring and the cyclohexane ring yields an energetically permitted conformation, whose pharmacophore groups can be superimposed on those of the template. Analogous compounds, which only differ in the length of the side chain at C-4' (**19**, **20**, **22**, **23**, **24**, **25**) or by an additional substituent at C-4 (**27**, **28**, **30**), were derived from this effective conformation of **21**. Compounds **28** and **30** differ from the prototype **21** in possessing an additional effect-increasing hydroxypropyl or hydroxybutyl side chain at C-4. The rigid compound **15** serves as template for orientation of the hydroxypropyl and hydroxybutyl side chains. Systematic conformational analysis was used to select a conformation of these side chains in which the alcoholic OH group was spatially in the neighbourhood of the pyran oxygen of the template. These conformations of **28** and **30** have a similar charge distribution to that of the template; this can be made visible in the form of the isopotential surface (Fig. 2). Since the charge distribution plays an important role during the approach of a molecule to the receptor, a similar charge distribution in the effective conformation of all active cannabinoids is required so that they can attach to the receptor at all. Compound **26** is a diastereomer of compound **27**, whose asymmetric C-1 has the absolute configuration *S*. Compound **27** and the prototype of the non-classical cannabinoids **21** exhibit an *R* configuration at C-1. Compound **26** can only fulfil the requirements of the pharmacophore in a conformation with ring C in the twist conformation, having all three substituents at the cyclohexane ring in a pseudo-equatorial position. Compound **29** is the enantiomer of **28**, a very active cannabinoid. Compound **29** exhibits only a slight affinity for the cannabinoid receptor. Systematic conformation analysis revealed a conformation of **29** that fitted the pharmacophore model. The cyclohexane ring lies in a chair conformation with all substituents positioned equatorially, as in the effective conformation of the very active enantiomer **28**. There were two possible ways in which the lowest energy conformation of **31**, with a torsional angle of ~44° between the cyclohexene ring and the aromatic ring, could be fitted to the template: that is, 2'-OH overlayed with 1-OH from the template molecule and, similarly, 6'-OH with 1-OH (here designated as superposition 1 and superposition 2, respectively).

In the pharmacophore model (Fig. 3), the oxygen of the phenolic OH group lies between 0.179 Å below and 0.264 Å above the plane of the aromatic of template **15** with a distance of 2.73–2.90 Å from the centroid of the aromatic of template **15**. The oxygen of the OH group at C-1 of the non-classical bicyclic cannabinoids and at C-9/C-11 of the classical cannabinoids lies 2.50–3.49 Å above the plane of the aromatic at a distance of 6.11–6.50 Å from the centroid. The oxygen of the additional effect-amplifying hydroxypropyl or hydroxybutyl side chain at C-4 of the non-classical bicyclic cannabinoids lies 0.80–0.85 Å below the plane of the aromatic and at a distance of 3.28–3.48 Å from the centroid.

YAK

The pseudoreceptor consists of 17 amino acid residues (His-Leu; Leu-Val; Asp; Phe-Phe-Phe; Phe-Phe; Phe-Phe; His-Trp; His; Leu-Leu) and is shown in Fig. 4; experimental and corrected free energies of ligand binding are compared in Table 2. During construction of the receptor model, it was found that increasing the hydrophobic

TABLE 3
CoMFA ANALYSIS BASED ON THE PHARMACOPHORE ALIGNMENT

No. of components	r^2_{cross}	r^2
5	0.630	0.977
4	0.576	0.958
3	0.541	0.927
2	0.399	0.825

content of the model in the region associated with the alkyl side chain increased the correlation coefficient for $\Delta(\Delta G^{\circ}_{exp.})$ versus $\Delta(\Delta G^{\circ}_{corr.})$ significantly. This is undoubtedly due to the clearly defined requirements for cannabinoid side-chain length and/or branching for receptor affinity (cf. above and below). Hence the use of phenyl residues because of their hydrophobicity and bulk. In general, the phenolic A ring hydroxyl acts as a hydrogen bond donor with an aspartate residue; the C ring hydroxyl also acts as a hydrogen donor but with a histidine residue. A histidine residue also interacts with the ether oxygen of the B ring as a hydrogen bond donor, but as a hydrogen bond acceptor with the hydroxypropyl or hydroxybutyl group of **28**–**30**. The amino moiety of **18** has interactions with two histidine residues, one of which serves as a hydrogen bond donor and the other as an acceptor. It is not proposed that this model structurally resembles the true biological receptor since the role of a pseudoreceptor is merely to reproduce relative energies of ligand binding. No information is available from mutation studies, so that it is not possible to construct the CB1-pseudoreceptor model from amino acids that are known to be essential for activity. However, all the amino acids selected are part of the known primary sequence of the CB1-receptor.

TABLE 4
CROSS-VALIDATED CoMFA ANALYSIS BASED ON THE PHARMACOPHORE ALIGNMENT; $r^2_{cross} = 0.630$, s_{pred} [a] = 0.792, F[b] = 7.845

Ligand	$\Delta G_{exp.}$ (kcal/mol)	$\Delta G_{calc.}$ (kcal/mol)	$\Delta G_{calc.} - \Delta G_{exp.}$ (kcal/mol)
15	–12.962	–12.971	0.009
28	–12.815	–12.086	0.729
18	–12.730	–11.241	1.489
30	–12.496	–12.638	–0.142
14	–12.480	–13.010	–0.530
22	–11.809	–10.818	0.991
26	–11.647	–11.364	0.283
27	–11.509	–11.557	–0.048
8	–11.503	–11.185	0.318
21	–11.377	–11.259	0.118
9	–10.924	–10.299	0.625
17	–10.854	–11.178	–0.324
23	–10.702	–10.230	0.472
3	–10.519	–9.910	0.609
1	–10.483	–9.828	0.655
13	–10.299	–10.152	0.147
10	–10.275	–11.014	–0.739
29	–10.227	–12.251	–2.024
2	–10.011	–10.363	–0.352
11	–10.001	–10.127	–0.126
12	–9.887	–10.524	–0.637
4	–9.797	–9.720	0.077
20	–9.787	–10.383	–0.596
6	–9.787	–10.087	–0.300
24	–9.628	–10.233	–0.605
5	–9.599	–10.353	–0.754
16	–9.400	–9.795	–0.395
25	–9.105	–10.205	–1.100
19	–8.700	–9.645	–0.945

[a] Standard error of predictions.
[b] Ratio of r^2 explained to unexplained = $r^2/(1-r^2)$.

TABLE 5
CoMFA ANALYSIS BASED ON THE PSEUDORECEPTOR ALIGNMENT

No. of components	r^2_{cross}	r^2
5	0.788	0.985
4	0.742	0.978
3	0.639	0.955
2	0.487	0.870

TABLE 6
CROSS-VALIDATED CoMFA ANALYSIS BASED ON THE PSEUDORECEPTOR ALIGNMENT; $r^2_{cross} = 0.788$, s_{pred} [a] = 0.603, F[b] = 17.085

Ligand	$\Delta G_{exp.}$ (kcal/mol)	$\Delta G_{calc.}$ (kcal/mol)	$\Delta G_{calc.} - \Delta G_{exp.}$ (kcal/mol)
15	–12.962	–12.965	–0.003
28	–12.815	–12.397	0.418
18	–12.730	–11.186	1.544
30	–12.496	–12.743	–0.247
14	–12.480	–11.646	0.834
22	–11.809	–11.543	0.266
26	–11.647	–11.079	0.568
27	–11.509	–11.484	0.025
8	–11.503	–11.058	0.445
21	–11.377	–11.509	–0.132
9	–10.924	–10.588	0.336
17	–10.854	–12.007	–1.153
23	–10.702	–10.690	0.012
3	–10.519	–10.103	0.416
1	–10.483	–10.012	0.471
13	–10.299	–10.510	–0.211
10	–10.275	–10.070	0.205
29	–10.277	–10.921	–0.644
2	–10.011	–10.835	–0.824
11	–10.001	–10.393	–0.392
12	–9.887	–9.846	–0.041
4	–9.797	–10.235	–0.438
20	–9.787	–9.764	–0.023
6	–9.787	–10.322	–0.535
24	–9.628	–9.893	–0.265
5	–9.599	–9.793	–0.194
16	–9.400	–9.491	–0.091
25	–9.105	–9.624	–0.519
19	–8.700	–9.269	–0.569

[a,b] As in Table 4.

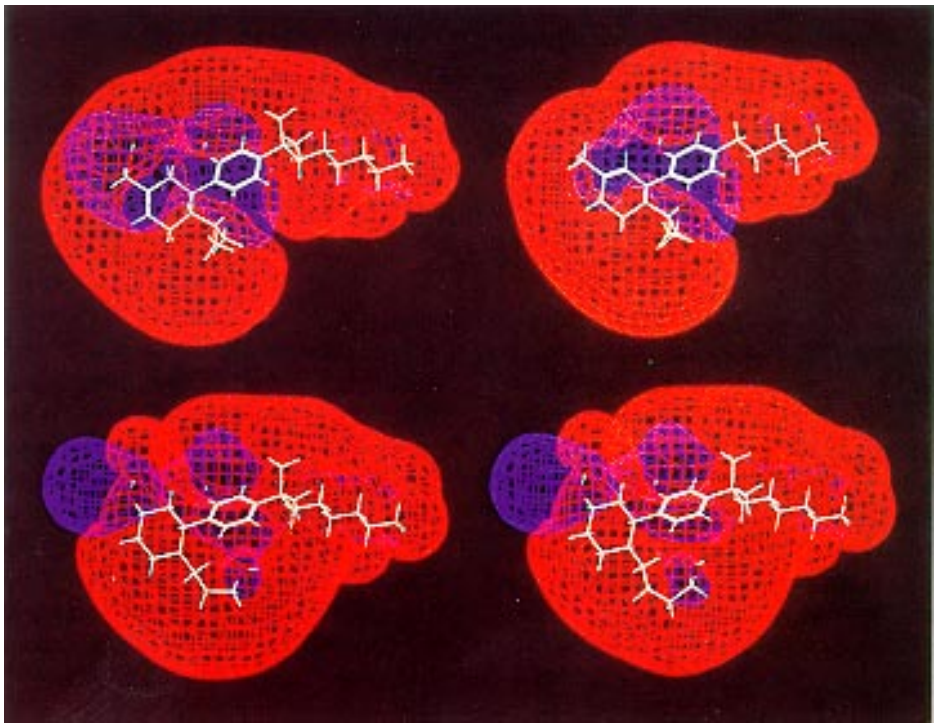

Fig. 2. Molecular electrostatic potentials derived from charge calculations using the semiempirical AM1 method contoured at −1.0 (blue) and 1.0 (red) kcal/mol: compounds **15** (top, left); **1** (top, right); **28** (bottom, left); **30** (bottom, right).

Of the 31 ligands, 29 were used at various stages to refine the receptor model; thus, the only two test ligands were **7** and **31**. For the training set, the correlation coefficient for $\Delta(\Delta G^{\circ}_{exp.})$ versus $\Delta(\Delta G^{\circ}_{corr.})$ is 0.951, indicating a good agreement between the calculated and experimental differences in the free energy of ligand binding (Fig. 5). After linear regression, the rms deviation of the calculated and experimental differences in the free energies for the training set $\Delta(\Delta G^{\circ})$ is 0.4 kcal/mol. Ligands **7** and **31** were then added to the pseudoreceptor model and refined in both position and orientation. The conformation of the pseudoreceptor was not altered in order to obtain the $\Delta(\Delta G^{\circ})$ value towards the receptor model. The predicted $\Delta(\Delta G^{\circ})$ of **7** relative to **15** of 1.93 kcal/mol compares to the experimental value of 1.45 kcal/mol. The pseudoreceptor model has a clear conformational preference for **31** (cf. above), a significantly closer agreement between experimental and predicted free energy binding values being achieved for superposition 2. The $\Delta(\Delta G^{\circ})$ of **31** relative to **15** of 8.94 and 5.09 kcal/mol for superpositions 1 and 2, respectively, compares to the experimental value of 5.36 kcal/mol. The 2'-OH of **31** (superposition 2) is able to

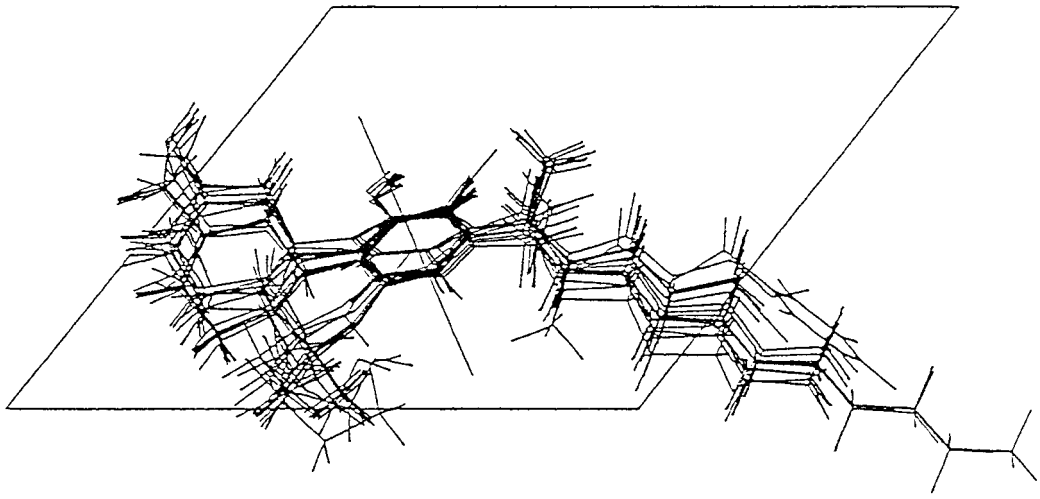

Fig. 3. Pharmacophore alignment of the 29 cannabinoid ligands (training set). Conformations of the molecules correspond to their alignment geometries of the pharmacophore model.

mimic the interactions of the amino moiety of **18**, the oxygen and hydrogen serving as a hydrogen bond acceptor and donor, respectively, with two histidine residues; no hydrogen bonds are made by the receptor with superposition 1 of **31**.

The dimethylheptyl ligands The ligands in question are **15**, **28**, **30**, **14**, **26**, **27**, **21**, **17** and **29**. These ligands have the side chain that confers maximal receptor affinity; however, they vary in the number and type of their hydrogen bonding moieties. The first four ligands span an experimental relative free energy range of ~0.5 kcal/mol and should be clearly distinguishable from **26**, **27** and **21**, which in turn should have very similar values with respect to each other (cf. Table 2). This is the case, but the difference in free binding energy between **26**, **27** and **21** with respect to **17** and **29** is not as clearly defined as it ought to be, since the free binding energies of the latter two ligands are overestimated, but those of the former three are underestimated.

Effect of side-chain length on binding affinity The ligands **19**, **20** and **22**–**25** have branched side chains of carbon length five, six, eight, nine, ten and eleven, respectively, and all lack the B ring of the primary ligand. Satisfyingly, the experimental ranking within this series of **22** > **23** > **20** > **24** > **25** and **25** > **19** is correctly reproduced by our pseudoreceptor model, although the ranks of **25** and **19** are reversed. Ligands having too short side chains (**19** and **20**) are unable to achieve good vdW interactions within the hydrophobic pocket, in contrast to **22**. The too long side chains of **24** and **25** are effectively forced out of the hydrophobic pocket, consequently weakening hydrogen bonding at the other end of the pseudoreceptor; the non-phenyl hydroxyl group of **25** does not participate in hydrogen bonding. In the case of **23**, which has a carbon side-chain length of nine (unfavourable), it is clear that the receptor model is too optimal. Excellent vdW interactions with phenyl residues of the receptor model are achieved via the C9' atom.

Ligands possessing non-complex side chains of carbon length five Within the series of ligands **3**, **13**, **4** and **5**, ranks are correctly reproduced. The ligands **7**–**10**, **1**, **2**, **11**, **12**, **6** and **16** also have unbranched side chains of carbon length five but lack the C ring hydroxyl. Of the three that are halogenated at the 5' terminal end (**7**, **8** and **10**), **10** is correctly calculated to have the poorest free binding energy (cf. Table 2). The computed free binding energy difference between **9** and **10** is eroded compared to the experimental value, although the ranking of these ligands relative to each other is consistent with the experimental order. The ranks of **1** and **10** are inverted, but the experimental difference in their $\Delta(\Delta G^\circ)$ values is only 0.21 kcal/mol. The remaining five ligands of this series span an experimental $\Delta(\Delta G^\circ)$ range of 0.6 kcal/mol. Ligand **2**, which should have the best free binding energy of the subseries, is in fact calculated to have a lesser binding energy than **16**, the ligand that should have the worst.

Fig. 4. Graphical representation of the YAK generated cannabinoid pseudoreceptor–ligand complex, showing ligand/pseudoreceptor interactions. Broken lines indicate electrostatic (green) and van der Waals (blue) interactions of the 29 cannabinoids (training set) with the pseudoreceptor.

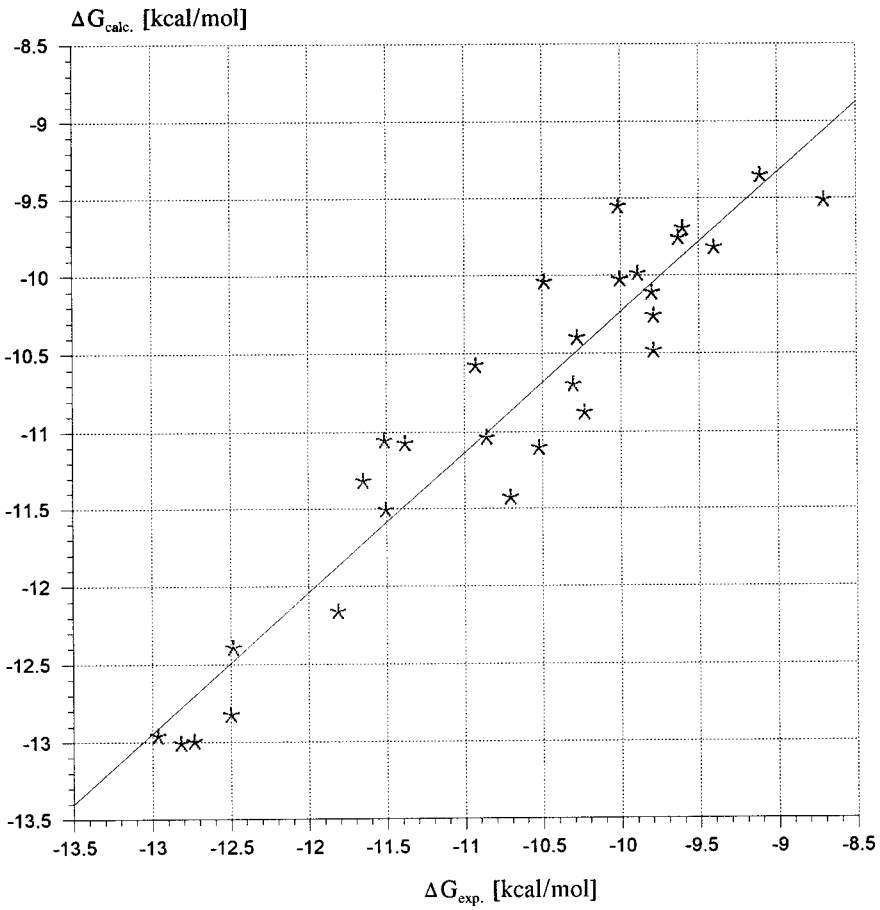

Fig. 5. Comparison of YAK computed and experimental free binding energies of the cannabinoid ligands (kcal/mol) (ΔΔG plot).

The spread of experimental Δ(ΔG°) for **11**, **12** and **6** is only 0.2 kcal/mol. This is reflected in the similarity of the calculated values for **11** and **12** (cf. Table 2); in comparison the Δ(ΔG°) value for **6** is underestimated.

Ligand **18** does not fit into any of the above categories, but is clearly identified as being one of the best ligands in terms of free binding energy (cf. Table 2).

CoMFA

The results of the first CoMFA analysis, the alignment of which is based on the pharmacophore model and will be addressed below as pharmacophore alignment, are listed in Table 3. The 29 cannabinoids subjected to the leave-one-out cross-validated CoMFA study with five components (Table 4, Fig. 6) included an outlier (**29**) with a deviation of 2.02 kcal/mol from the experimental free binding energy value. Compound **18**, which differs structurally from the other cannabinoids in the side chain at C-3 and in the exchange of the benzochromene oxygen for a nitrogen, was poorly predicted in the cross-validated CoMFA analysis (deviation of 1.489 kcal/mol). In the case of three further synthetic cannabinoids that only differed in the length of the side chain (**19**, **22**, **25**), the cross-validated CoMFA analysis did not reflect satisfactorily the influence of the length/branching of the side chain on the activity of the cannabinoids at the receptor, whereby hydrophobic interactions and steric effects play an important role.

The results of the second CoMFA study, based on the new alignment obtained from the pseudoreceptor, are summarized in Table 5. The 29 cannabinoids analysed do not contain any more compounds with a deviation of >2.0 kcal/mol from the experimental value in the leave-one-out cross-validated CoMFA analysis with five components (Table 6, Fig. 7). In contrast to the first CoMFA analysis, compound **29**, the enantiomer of **28**, is no longer an outlier. Only two compounds have deviations >1.0 kcal/mol; these include, as in the CoMFA analysis with pharmacophore alignment, compound **18**, but in addition also **17**, which differs structurally from the other cannabinoids. The prediction for the side-chain analogues of the non-classical bicyclic cannabinoids was unequivocally improved using the YAK alignment. The second CoMFA model is significantly more stable; it not only has better r^2_{cross} values but also yields good r^2_{cross} levels on reduction of the components. The first CoMFA model had an r^2_{cross} value of 0.630 with five components, while the second CoMFA model yielded a comparable r^2_{cross} value of 0.639

with only three components. Figure 8 shows the 3D coefficient contour map of the second final CoMFA analysis.

The final PLS analysis of the complete data set serves for the prediction of new compounds. The final non-cross-validated CoMFA model based on the pharmacophore alignment including 29 cannabinoids has an r^2 value of 0.977 (Table 7) and thus reveals a good agreement between the experimental and calculated free energies of binding as does the final non-cross-validated CoMFA model based on the pseudoreceptor alignment, r^2 value of 0.985 ($r = 0.991$, Table 8). The largest deviation from the experimental value ($\Delta G_{exp.}$) is 0.347 kcal/mol. The predicted free binding energies of **7** and **31** are slightly more in accord with experimental values in the CoMFA analysis based on the pharmacophore alignment than the pseudoreceptor alignment. Superposition 1 of **31** yields better results in both final CoMFA analyses.

Discussion and Conclusions

The hypothetical nature of the model is to be explicitly emphasized, since the model has been established solely on the basis of the properties of the ligands. However, a close approach to reality is indicated, on the one hand, by the good correlation with experimental binding data and, on the other hand, by the consistency between structure–effect relationships, pharmacophore model, pseudoreceptor model and CoMFA model. The pseudoreceptor yields a refined pharmacophore and simulates ligand–receptor interactions in the active centre at the molecular level. The essential side chain of the cannabinoids provides a large contribution to the energy of interaction between ligand and receptor in the form of hydrophobic interactions. This contribution confirms the essential importance of the side chain for the affinity of the receptor [2] and it is possible to conclude that the receptor involves a hydrophobic pocket in which the side chain is bound by hydrophobic interactions. The influence of the length of the side chain on the binding affinity provides information concerning the depth of the hydrophobic pocket. Cannabinoids with shorter side chains fit into this pocket, but exhibit smaller hydrophobic interactions. Cannabinoids with longer side chains exhibit good hydrophobic interactions, but beyond a certain limit their volume can no longer be accommodated by the pocket, so that there is a weakening in the binding affinity as a result of a reduction in the energetically favourable geometrical optimal

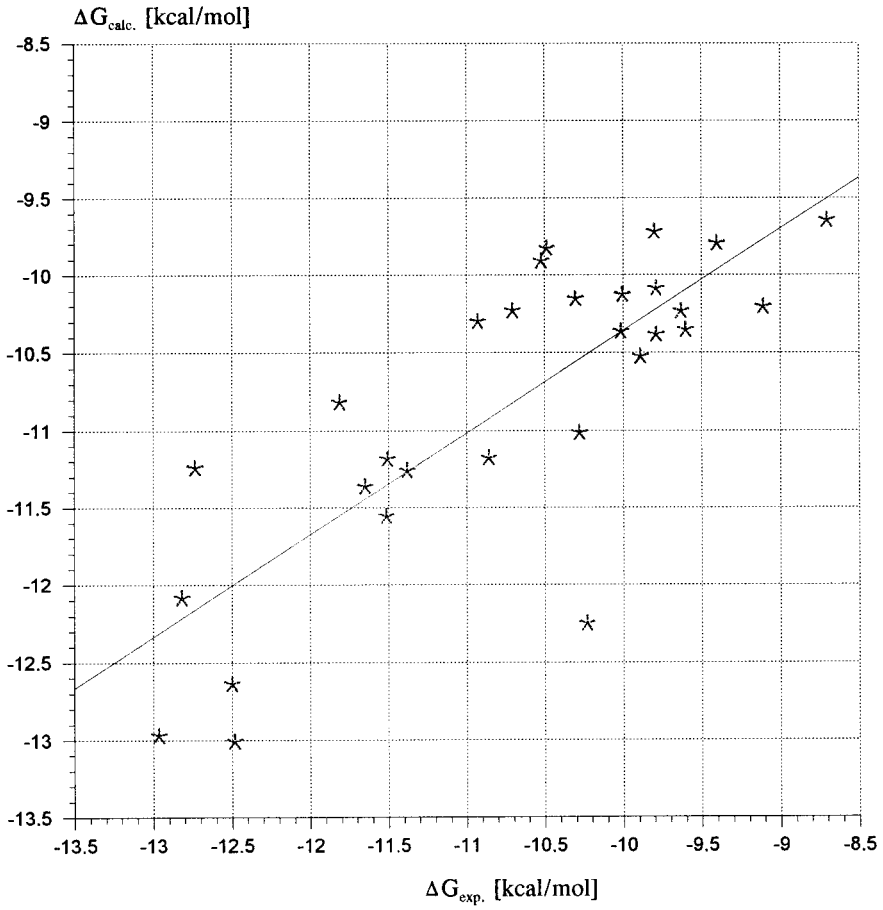

Fig. 6. Cross-validated CoMFA analysis with five components based on the pharmacophore alignment; $r^2_{cross} = 0.630$.

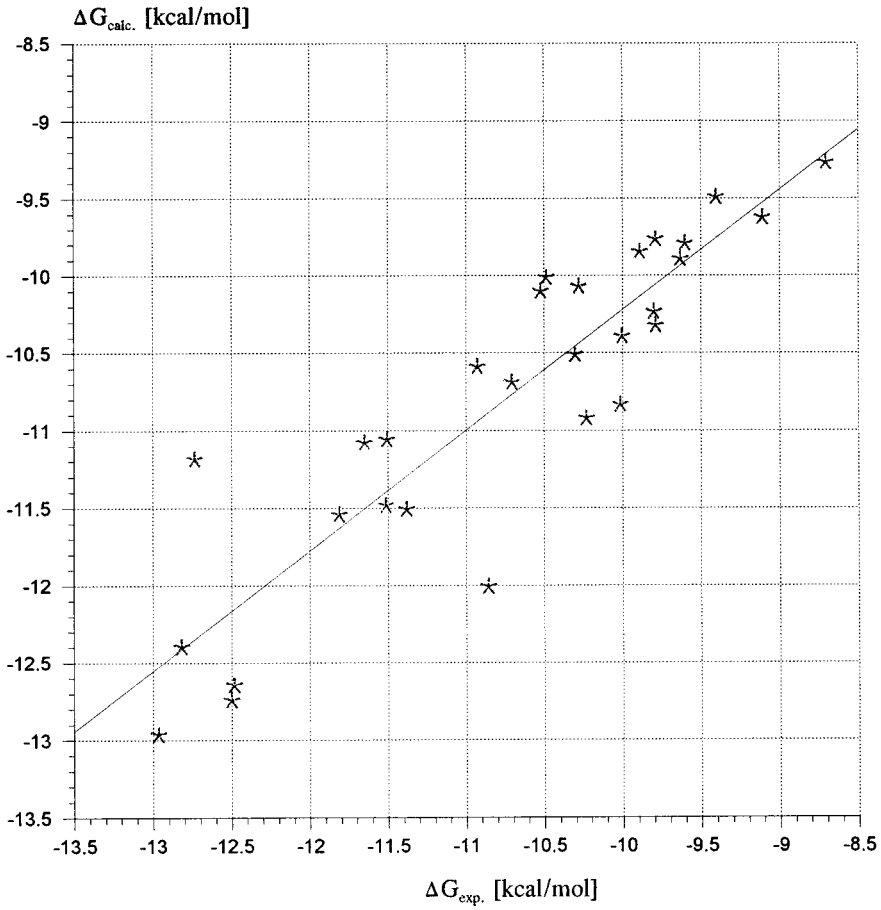

Fig. 7. Cross-validated CoMFA analysis with five components based on the pseudoreceptor alignment; $r^2_{cross} = 0.788$.

interactions. These results point to the structural requirements of the length and/or branching of the alkyl side chain for the receptor affinity [39]. Additionally, hydrogen bonds play an important role in the binding of the cannabinoids to the biological receptor. An energetically favourable, geometrically optimal hydrogen bond between

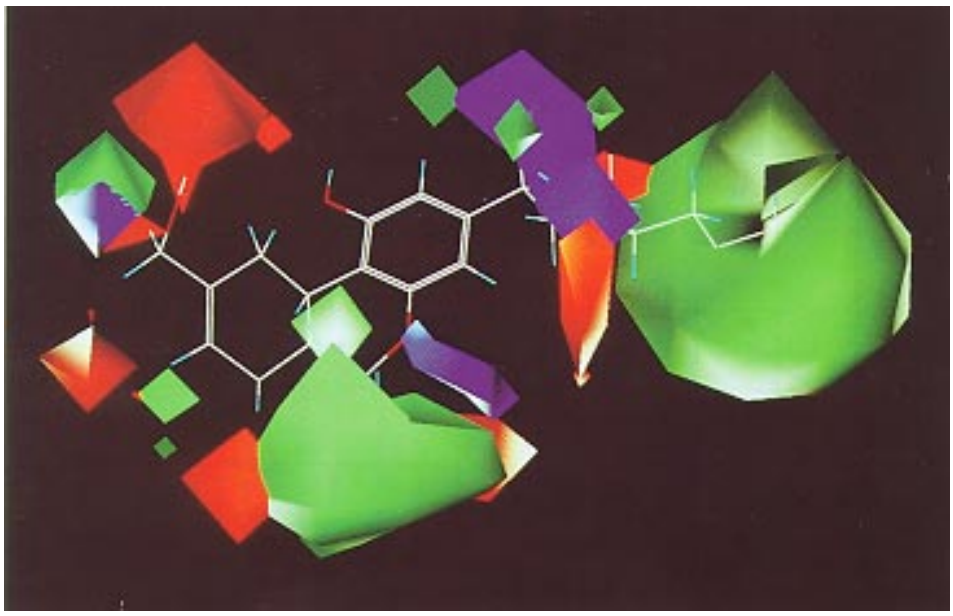

Fig. 8. Coefficient contour map of the second CoMFA analysis. Substituents in the green regions increase the binding affinity. Positive charges in blue regions and negative charges in red regions increase the binding affinity.

TABLE 7
FINAL NON-CROSS-VALIDATED CoMFA ANALYSIS BASED ON THE PHARMACOPHORE ALIGNMENT

Ligand	$\Delta G_{exp.}$ (kcal/mol)	$\Delta G_{calc.}$ (kcal/mol)	$\Delta G_{calc.} - \Delta G_{exp.}$ (kcal/mol)
Training set[a]			
15	–12.962	–13.141	–0.179
28	–12.815	–12.660	0.155
18	–12.730	–12.798	–0.068
30	–12.496	–12.608	–0.112
14	–12.480	–12.640	–0.160
22	–11.809	–11.383	0.426
26	–11.647	–11.609	0.038
27	–11.509	–11.628	–0.119
8	–11.503	–11.307	0.196
21	–11.377	–11.321	0.056
9	–10.924	–10.912	0.012
17	–10.854	–10.645	0.209
23	–10.702	–10.524	0.178
3	–10.519	–10.658	–0.139
1	–10.483	–10.354	0.129
13	–10.299	–10.351	–0.052
10	–10.275	–10.300	–0.025
29	–10.227	–10.026	0.201
2	–10.011	–10.217	–0.206
11	–10.001	–9.868	0.133
12	–9.887	–9.908	–0.021
4	–9.797	–9.610	0.187
20	–9.787	–10.073	–0.286
6	–9.787	–9.907	–0.120
24	–9.628	–10.037	–0.409
5	–9.599	–9.458	0.141
16	–9.400	–9.303	0.097
25	–9.105	–9.212	–0.107
19	–8.700	–9.015	–0.315
Test set			
7	–11.514	–11.121	0.393
31	–7.605	–7.738[b]	–0.133[b]
		–8.280[c]	–0.675[c]

[a] The training set contains 29 ligands; $r^2 = 0.977$, standard error of estimate $s_{est} = 0.197$, F = ratio of r^2 explained to unexplained (= $r^2/(1-r^2)$) = 197.572.
[b] Superposition 1.
[c] Superposition 2.

the essential phenolic hydroxyl group and a hydrophilic amino acid of the receptor is common to all ligands. The participation of the phenolic proton in the receptor–ligand interaction is in agreement with the molecular modelling studies of Semus [40]. In addition, a hydrogen bond is also formed between the hydroxyl group at C-9/C-11 (classical cannabinoids) or C-1 (non-classical cannabinoids) and a further hydrophilic amino acid at the receptor.

Both the CoMFA and pseudoreceptor methods predicted free energies of ligand binding for the test ligands that were in good agreement with the experimental values; in this respect, neither method can be said to be superior to the other. However, based upon the functionality of groups in the ligands and the directionality of molecular interactions, explicit interactions exist between the ligands with the pseudoreceptor model. Thus, the generation of rationalizations concerning structure–activity relationships may be facilitated in comparison to CoMFA. However, our study has unequivocally shown the superiority of a combined approach using YAK and CoMFA. While one of the severe problems in CoMFA is the proper alignment of the ligands, YAK turned out to be an excellent tool to provide a realistic alignment based on $\Delta\Delta G$ correlation. Thus, the considerable improvement of CoMFA analysis by using the YAK alignment is one of the significant results of our study and may have general importance as a suggestion for further approaches to this area of research.

Of course, we know that a model containing 17 amino acids is very likely to be statistically weak. However, pseudoreceptor models from YAK may not be mixed up

TABLE 8
FINAL NON-CROSS-VALIDATED CoMFA ANALYSIS BASED ON THE PSEUDORECEPTOR ALIGNMENT

Ligand	$\Delta G_{exp.}$ (kcal/mol)	$\Delta G_{calc.}$ (kcal/mol)	$\Delta G_{calc.} - \Delta G_{exp.}$ (kcal/mol)
Training set[a]			
15	–12.962	–13.117	–0.155
28	–12.815	–12.783	0.032
18	–12.730	–12.872	–0.142
30	–12.496	–12.635	–0.139
14	–12.480	–12.433	0.047
22	–11.809	–11.703	0.106
26	–11.647	–11.479	0.168
27	–11.509	–11.507	0.002
8	–11.503	–11.197	0.306
21	–11.377	–11.422	–0.045
9	–10.924	–11.020	–0.096
17	–10.854	–10.751	0.103
23	–10.702	–10.662	0.040
3	–10.519	–10.327	0.192
1	–10.483	–10.174	0.309
13	–10.299	–10.415	–0.116
10	–10.275	–10.144	0.131
29	–10.227	–10.162	0.065
2	–10.011	–10.137	–0.126
11	–10.001	–10.093	–0.092
12	–9.887	–9.812	0.075
4	–9.797	–9.791	0.006
20	–9.787	–9.712	0.075
6	–9.787	–10.134	–0.347
24	–9.628	–9.620	0.008
5	–9.599	–9.686	–0.087
16	–9.400	–9.453	–0.053
25	–9.105	–9.209	–0.104
19	–8.700	–8.864	–0.164
Test set			
7	–11.514	–10.813	0.701
31	–7.605	–8.169[b]	–0.564[b]
		–8.593[c]	–0.988[c]

[a] The training set contains 29 ligands; $r^2 = 0.985$, $s_{est} = 0.161$, F = ratio of r^2 explained to unexplained (= $r^2/(1-r^2)$) = 299.920.
[b] Superposition 1.
[c] Superposition 2.

with 3D-QSAR techniques. The 17 amino acids in a pseudoreceptor model have different quality in describing the pharmacophoric interactions compared to a statistical distribution of amino acids, because of the rule-based choice of ligands. The rules stem from a careful evaluation of X-ray data of protein–ligand interaction complexes. Molecular modelling is an essential part of the pseudoreceptor technique. Each amino acid placed by the system is only a suggestion and is normally optimized by the user by a knowledge-driven process based on data from biochemistry and biophysics of the target protein and the ligand kinetics. Thus, including the quite satisfying thermodynamic correlation, the 17 amino acid pseudoreceptor model represents a robust model of the cannabinoid interaction site.

References

1 Gaoni, Y. and Mechoulam, R., J. Am. Chem. Soc., 93 (1971) 217.
2 Razdan, R.K., Pharmacol. Rev., 38 (1986) 75.
3 Kovar, K.-A., Pharm. Unserer Zeit, 3 (1981) 65.
4 Kovar, K.-A., Dtsch. Apoth. Ztg., 43 (1992) 2302.
5 Schmidbauer, W. and Scheidt, J., Handbuch der Rauschdrogen, 6th ed., Nymphenburger Verlag, München, Germany, 1981.
6 Mechoulam, R. and Lander, N., Pharm. Int., 1 (1980) 19.
7 Compton, D.R., Rice, K.C., DeCosta, B.R., Razdan, R.K., Melvin, L.S., Johnson, M.R. and Martin, B.R., J. Pharmacol. Exp. Ther., 265 (1993) 218.
8 Martin, W.J., Patrick, S.L., Coffin, P.O., Tsou, K. and Walker, J.M., Life Sci., 56 (1995) 2103.
9 Johnson, M.R., Melvin, L.S., Althuis, T.H., Bindra, J.S., Harbert, C.A., Milne, G.M. and Weissman, A., J. Clin. Pharmacol., 21 (1981) 271.
10 Johnson, M.R. and Melvin, L.S., In Mechoulam, R. (Ed.) Cannabinoids as Therapeutic Agents, CRC Press, Boca Raton, FL, U.S.A., 1986, pp. 121–146.
11 Reggio, P.H., Seltzman, H.H., Compton, D.R., Prescott, W.R., Martin, J.R. and Martin, B.R., Mol. Pharmacol., 38 (1990) 854.
12 Little, P.J., Compton, D.R., Mechoulam, R. and Martin, B.R., Biochem. Behav., 32 (1989) 661.
13 Thomas, B.F., Compton, D.R., Martin, B.R. and Semus, S.F., Mol. Pharmacol., 40 (1991) 656.
14 Howlett, A.C., Johnson, M.R., Melvin, L.S. and Milne, G.M., Mol. Pharmacol., 33 (1988) 297.
15 Reggio, P.H., Panu, A.M. and Miles, S., J. Med. Chem., 36 (1993) 1761.
16 Makriyannis, A. and Rapaka, R.S., Life Sci., 47 (1990) 2173.
17 Devan, W.A., Dysarz, F.A., Johnson, M.R., Melvin, L.S. and Howlett, A.C., Mol. Pharmacol., 34 (1988) 605.
18 Matsuda, L.A., Lolait, S.J., Brownstein, M.J., Young, A.C. and Bonner, T.J., Nature, 346 (1990) 561.
19 Sean, M., Kerrie, L.T. and Muna, A.-S., Nature, 365 (1993) 61.
20 Compton, D.R., Johnson, M.R., Melvin, L.S. and Martin, B.R., J. Pharmacol. Exp. Ther., 260 (1992) 201.
21 Cambridge Crystallographic Database, Crystallographic Data Centre, University Chemical Laboratory, Cambridge, U.K.
22 Stewart, J.J.P., MOPAC 5.0. A general molecular orbital package (QCPE 455), Frank J. Seiler Research Laboratory, Colorado Springs, CO, U.S.A.
23 Briem, H., Dissertation, Berlin, Germany, 1990.
24 Archer, R.A., Boyd, D.B., Demarco, P.V., Tyminski, L.J. and Allinger, N.L., J. Am. Chem. Soc., 92 (1970) 5200.
25 Reggio, P.H. and Mazurek, A.P., J. Mol. Struct. (THEOCHEM), 149 (1987) 331.
26 Kriwacki, R.W. and Makriyannis, A., Mol. Pharmacol., 35 (1989) 495.
27 Sufrin, J.R., Dunn, D.A. and Marshall, G.R., Mol. Pharmacol., 19 (1980) 307.
28 Marshall, G.R., Barry, C.D., Bosshard, H.E., Dammkoehler, R.A. and Dunn, D.A., Comput. Assisted Drug Design, 112 (1979) 205.
29 Marshall, G.R. and Motoc, J., In Burgen, A.S.V., Roberts, G.C.K. and Tute, M.S. (Eds.) Molecular Graphics and Drug Design, Elsevier, Amsterdam, The Netherlands, 1986, pp. 115–156.
30 Marshall, G.R. and Cramer III, R.D., Trends Pharmacol. Sci., 9 (1988) 285.
31 Hibert, M.F., Gittos, M.W., Middlemiss, D.N., Mir, A.K. and Fozard, J.R., J. Med. Chem., 31 (1988) 1087.
32 Vedani, A., Zbinden, P., Snyder, J.P. and Greenidge, P.A., J. Am. Chem. Soc., 117 (1995) 4987.
33 Still, W.C., Tempczyk, A., Hawley, R.C. and Hendrickson, T.J., J. Am. Chem. Soc., 112 (1990) 6127.
34 Thibaut, U., Folkers, G., Klebe, G., Kubinyi, H., Merz, A. and Rognan, D., In Kubinyi, H. (Ed.) 3D QSAR in Drug Design: Theory, Methods and Applications, ESCOM, Leiden, The Netherlands, 1993, pp. 711–716.
35 Rosenqvist, E. and Otterson, T., Acta Chem. Scand., B29 (1975) 379.
36 Tollenaere, J.P., Moereels, H. and Raymaekers, L.A., Atlas of the Three-dimensional Structure of Drugs, Elsevier, Amsterdam, The Netherlands, 1979, p. 232.
37 Binder, M., Edery, H. and Porath, G., In Nahas, G.G. and Paton, W.D.M. (Eds.) Marihuana Biological Effects, Analysis, Metabolism, Cellular Responses, Reproduction and Brain, Pergamon, Oxford, U.K., 1979, pp. 71–80.
38 Xie, X.-Q., Yang, D.-P., Melvin, L.S. and Makriyannis, A., J. Med. Chem., 37 (1994) 1418.
39 Thomas, B.F., Compton, D.R., Martin, B.R. and Semus, S.F., Mol. Pharmacol., 40 (1991) 656.
40 Semus, S.F., Med. Chem. Res., 1 (1992) 454.